7-29-2013

Accuracy improvement of quantitative analysis by spatial confinement in laser-induced breakdown spectroscopy

L. B. Guo
Huazhong University of Science and Technology,University of Nebraska-Lincoln

Z. Q. Hao
Huazhong University of Science and Technology

M. Shen
Huazhong University of Science and Technology

W. Xiong
University of Nebraska-Lincoln

X. N. He
University of Nebraska-Lincoln

See next page for additional authors

Accuracy improvement of quantitative analysis by spatial confinement in laser-induced breakdown spectroscopy

L.B. Guo,[1,2] Z.Q. Hao,[1] M. Shen,[1] W. Xiong,[2] X.N. He,[2] Z.Q. Xie,[2] M. Gao, [1,*] X.Y. Li,[1] X.Y. Zeng,[1] and Y.F. Lu[2]

[1]*Wuhan National Laboratory for Optoelectronics (WNLO), Huazhong University of Science and Technology, Wuhan, Hubei 430074, China*

[2]*Department of Electrical Engineering, University of Nebraska-Lincoln, Lincoln, NE 68588-0511, USA*

[*]*mgao@mail.hust.edu.cn*

Abstract: To improve the accuracy of quantitative analysis in laser-induced breakdown spectroscopy, the plasma produced by a Nd:YAG laser from steel targets was confined by a cavity. A number of elements with low concentrations, such as vanadium (V), chromium (Cr), and manganese (Mn), in the steel samples were investigated. After the optimization of the cavity dimension and laser fluence, significant enhancement factors of 4.2, 3.1, and 2.87 in the emission intensity of V, Cr, and Mn lines, respectively, were achieved at a laser fluence of 42.9 J/cm^2 using a hemispherical cavity (diameter: 5 mm). More importantly, the correlation coefficient of the V I 440.85/Fe I 438.35 nm was increased from 0.946 (without the cavity) to 0.981 (with the cavity); and similar results for Cr I 425.43/Fe I 425.08 nm and Mn I 476.64/Fe I 492.05 nm were also obtained. Therefore, it was demonstrated that the accuracy of quantitative analysis with low concentration elements in steel samples was improved, because the plasma became uniform with spatial confinement. The results of this study provide a new pathway for improving the accuracy of quantitative analysis of LIBS.

OCIS codes: (300.6365) Spectroscopy, laser induced breakdown; (350.5400) Plasmas; (020.6580) Stark effect.

References and links

1. L. J. Radziemski and D. A. Cremers, *Laser Induced Plasma and Applications* (Marcel Dekker, New York, 1989).
2. H. Zhang, F. Y. Yueh, and J. P. Singh, "Laser-induced breakdown spectrometry as a multimetal continuous-emission monitor," Appl. Opt. **38**(9), 1459–1466 (1999).
3. D. W. Hahn and M. M. Lunden, "Detection and analysis of aerosol particles by laser-induced breakdown spectroscopy," Aerosol Sci. Technol. **33**(1-2), 30–48 (2000).
4. J. P. Singh and S. N. Thakur, *Laser-Induced breakdown Spectroscopy*, (Elsevier Science, Oxford, 2007).
5. A. K. Knight, N. L. Scherbarth, D. A. Cremers, and M. J. Ferris, "Characterization of Laser-Induced Breakdown Spectroscopy (LIBS) for Application to Space Exploration," Appl. Spectrosc. **54**(3), 331–340 (2000).
6. A. W. Miziolect, V. Palleschi, and I. Schechter, eds., *Laser-Induced Breakdown Spectroscopy (LIBS) - Fundamentals and Applications*, (Cambridge University Press, Cambridge, 2006).
7. R. Noll, H. Bette, A. Brysch, M. Kraushaar, I. Mönch, L. Peter, and V. Sturm, "Laser-induced breakdown spectrometry — applications for production control and quality assurance in the steel industry," Spectrochim. Acta, B At. Spectrosc. **56**(6), 637–649 (2001).
8. U. Panne, R. E. Neuhauser, M. Theisen, H. Fink, and R. Niessner, "Analysis of heavy metal aerosols on filters by laser-induced plasma spectroscopy," Spectrochim. Acta, B At. Spectrosc. **56**(6), 839–850 (2001).
9. G. Arca, A. Ciucci, V. Palleschi, S. Rastelli, and E. Tognoni, "Trace element analysis in water by the laser-induced breakdown spectroscopy techinique," Appl. Spectrosc. **51**(8), 1102–1105 (1997).
10. T. X. Phuoc and F. P. White, "Laser induced spark for measurements of the fuel-to-air ratio of a combustible mixture," Fuel **81**(13), 1761–1765 (2002).
11. A. K. Knight, N. L. Scherbarth, D. A. Cremers, and M. J. Ferris, "Characterization of laser-induced breakdown spectroscopy (LIBS) for application to space exploration," Appl. Spectrosc. **54**(3), 331–340 (2000).

#191010 - $15.00 USD Received 22 May 2013; revised 6 Jul 2013; accepted 11 Jul 2013; published 22 Jul 2013

12. J. Scaffidi, J. Pender, W. Pearman, S. R. Goode, B. W. Colston, Jr., J. C. Carter, and S. M. Angel, "Dual-pulse laser-induced breakdown spectroscopy with combinations of femtosecond and nanosecond laser pulses," Appl. Opt. **42**(30), 6099–6106 (2003).
13. L. B. Guo, B. Y. Zhang, X. N. He, C. M. Li, Y. S. Zhou, T. Wu, J. B. Park, X. Y. Zeng, and Y. F. Lu, "Optimally enhanced optical emission in laser-induced breakdown spectroscopy by combining spatial confinement and dual-pulse irradiation," Opt. Express **20**(2), 1436–1443 (2012).
14. X. N. He, W. Hu, C. M. Li, L. B. Guo, and Y. F. Lu, "Generation of high-temperature and low-density plasmas for improved spectral resolutions in laser-induced breakdown spectroscopy," Opt. Express **19**(11), 10997–11006 (2011).
15. G. Asimellis, S. Hamilton, A. Giannoudakos, and M. Kompitsas, "Controlled inert gas environment for enhanced chlorine and fluorine detection in the visible and near-infrared by laser-induced breakdown spectroscopy," Spectrochimica Acta Part B. **60**(7-8), 1132–1139 (2005).
16. L. Li, Z. Wang, T. Yuan, Z. Hou, Z. Li, and W. Ni, "A simplified spectrum standardization method for laser induced breakdown spectroscopy measurements," J. Anal. At. Spectrom. **26**(11), 2274–2280 (2011).
17. Z. Y. Hou, Z. Wang, S. L. Lui, Z. Hou, T. B. Yuan, Z. Li, and W. Ni, "Improving data stability and prediction accuracy in laser-induced breakdown spectroscopy by utilizing a combined atomic and ionic line algorithm," J. Anal. At. Spectrom. **28**(107), 107–113 (2013).
18. N. B. Zorov, A. A. Gorbatenko, T. A. Labutin, and A. M. Popov, "A review of normalization techniques in analytical atomic spectrometry with laser sampling: From single to multivariate correction," Spectrochim. Acta, B At. Spectrosc. **65**(8), 642–657 (2010).
19. Q. L. Ma, V. Motto-Ros, W. Q. Lei, M. Boueri, X. S. Bai, L. J. Zheng, H. P. Zeng, and J. Yu, "Temporal and spatial dynamics of laser-induced aluminum plasma in argon background at atmospheric pressure: interplay with the ambient gas," Spectrochim. Acta, B At. Spectrosc. **65**(11), 896–907 (2010).
20. Q. L. Ma, V. Motto-Ros, F. Laye, J. Yu, W. Q. Lei, X. S. Bai, L. J. Zheng, and H. P. Zeng, "Ultraviolet versus infrared: effects of ablation laser wavelength on the expansion of laser-induced plasma into one-atmosphere argon gas," J. Appl. Phys. **111**(5), 053301 (2012).
21. H. Sobral, M. Villagrán-Muniz, R. Navarro-González, and A. C. Raga, "Temporal evolution of the shock wave and hot core air in laser induced plasma," Appl. Phys. Lett. **77**(20), 3158–3160 (2000).
22. M. Corsi, G. Cristoforetti, M. Hidalgo, D. Iriarte, S. Legnaioli, V. Palleschi, A. Salvetti, and E. Tognoni, "Effect of laser-induced crater depth in laser-induced breakdown spectroscopy emission features," Appl. Spectrosc. **59**(7), 853–860 (2005).
23. X. K. Shen, J. Sun, H. Ling, and Y. F. Lu, "Spectroscopic study of laser-induced Al plasmas with cylindrical confinement," J. Appl. Phys. **102**(9), 093301 (2007).
24. A. M. Popov, F. Colao, and R. Fantoni, "Enhancement of LIBS signal by spatially confining the laser-induced plasma," J. Anal. At. Spectrom. **24**(5), 602 (2009).
25. A. M. Popov, F. Colao, and R. Fantoni, "Spatial confinement of laser-induced plasma to enhance LIBS sensitivity for trace elements determination in soils," J. Anal. At. Spectrom. **25**(6), 837–848 (2010).
26. L. B. Guo, C. M. Li, W. Hu, Y. S. Zhou, B. Y. Zhang, Z. X. Cai, X. Y. Zeng, and Y. F. Lu, "Plasma confinement by hemispherical cavity in laser-induced breakdown spectroscopy," Appl. Phys. Lett. **98**(13), 131501 (2011).
27. L. B. Guo, W. Hu, B. Y. Zhang, X. N. He, C. M. Li, Y. S. Zhou, Z. X. Cai, X. Y. Zeng, and Y. F. Lu, "Enhancement of optical emission from laser-induced plasmas by combined spatial and magnetic confinement," Opt. Express **19**(15), 14067–14075 (2011).
28. Z. Wang, Z. Y. Hou, S. L. Lui, D. Jiang, J. M. Liu, and Z. Li, "Utilization of moderate cylindrical confinement for precision improvement of laser-induced breakdown spectroscopy signal," Opt. Express **20**(S6), A1011–A1018 (2012).
29. I. Bassiotis, A. Diamantopoulou, A. Giannoudakos, F. Roubani-Kalantzopoulou, and M. Kompitsas, "Effects of experimental parameters in quantitative analysis of steel alloy by laser-induced breakdown spectroscopy," Spectrochimica Acta Part B. **56**(6), 671–683 (2001).
30. L. I. Sedov, Similarity and Dimensional Methods in Mechanics (Cleaver Hume, London, 1959).

1. Introduction

The technique of laser-induced breakdown spectroscopy (LIBS) has been drawing unprecedented attention in recent years, due to its capabilities for rapid response, *in situ* elemental analysis with low invasiveness, and simultaneous multielement detection, normally without the need for sample preparation [1–6]. LIBS has already been applied in a wide range of applications, such as civilian and military environmental monitoring, cultural heritage analysis and characterization, and biological and medical identification, as well as space exploration [7–11]. However, one of the major drawbacks of LIBS is its low detection sensitivity in determining trace elements. To enhance the LIBS sensitivity, various approaches have been proposed to improve the analytical performance of the technique, such as controlling the atmosphere, multiple pulse excitation, introduction of inert gas [12–15], and spectra normalization [16–18].

The sensitivity of LIBS can be significantly improved using the methods described above [19,20]. However, there are two drawbacks: one is the increased complexity of the LIBS

#191010 - $15.00 USD Received 22 May 2013; revised 6 Jul 2013; accepted 11 Jul 2013; published 22 Jul 2013

setup, and the other is the increased cost of using more than one laser. Besides adding lasers or introducing gases, another simple, flexible, and cost-effective approach is plasma confinement, which can easily be used to improve the detection sensitivity of LIBS. Along with the generation and expansion of the laser-induced plasma in air, a shock wave would be generated. During the shock wave expansion, it would be reflected back when it encounters obstacles such as a plate wall or a cylindrical wall and would compress the plasma plume [21]. The compressed plasma would lead to an increased collision rate among the particles, resulting in an increased number of atoms in high-energy states and, hence, reheating and maintaining a higher temperature in the plasma to enhance the emission intensity. Different cavity configurations have been studied for their confinement effects in air. Corsi *et al.* created two different crater depths (1 mm in diameter, and 1 mm and 1.5 mm in depth) with a drill on a copper sample. It was shown that the confinement effect produced by the craters enhances the LIBS signal [22]. Shen *et al.* used a series of cylindrical pipes with different diameters to confine the plasma and showed that the maximum signal enhancement factor was about 9 [23]. Popov *et al.* reported the confinement effect of plasmas created in a small capped cylindrical chamber whose size was 4 mm by 4 mm, improved the limit of detection (LOD) by two to five times for different elements [24,25]. Our previous research also showed the enhancement of plasmas confined with an aluminum hemispherical cavity, resulting in an enhancement factor of 12 for Mn lines in a substrate with a low Mn concentration [26,27]. Wang *et al* fabricated a polytetrafluoroethylene (PTFE) plate of 1.5 mm thick with a diameter of 3 mm to regularize coal plasma. It was verified that the configuration both enhanced the spectral line intensity and reduced shot-to-shot fluctuation [28]. However, previous research focused mainly on the sensitivity improvement of elements with high concentrations using spatial confinement, i.e., their research priorities were on qualitative analysis but rarely on the accuracy of the quantitative analysis improvement as described above.

In this study, our main aim was to investigate the accuracy of the quantitative analysis improvement of low concentration elements with optical thin lines from LIBS measurement using spatial confining of plasmas, based on the enhancement of optical emission spectra of the plasmas.

2. Experimental methods

The schematic diagram of the experimental setup used in this study is shown in Fig. 1. The experiments were conducted in open air. A third harmonic Q-switched Nd:YAG laser (Quantel Brilliant, pulse duration: 5 ns) operating at 355 nm with a repetition rate of 10 Hz was used for plasma generation. The laser beam was reflected by a dichroic mirror and focused by a UV-grade quartz lens (focal length, 15 cm), through the 2-mm hole at the top of hemispherical cavities (aluminum, diameter: 5, 6, 7, and 8 mm) onto the steel targets. The reflection band of the dichroic mirror is from 345 to 404 nm, which reflects the laser beam but transmits the other wavelengths from the plasmas. Plasma plumes with a size of several millimeters were generated at the center of the hemisphere on top of the sample surface. The emission from the laser-induced plasmas were collected through the top hole, and coupled to an optical fiber by the UV-grade quartz lens and a light collector (Ocean Optics, 84-UV-25, wavelength range: 200–2000 nm). The optical fiber has a 50-μm core diameter with its output end connected to an echelle spectrometer (Andor Tech., Mechelle 5000). The wavelength range of the spectrograph is 200–950 nm with a spectral resolution of $\lambda/\Delta\lambda = 5000$. A 1024 × 1024 pixel intensified charge-coupled device (ICCD) (Andor Tech., iStar DH-334T) was attached to the exit focal plane of the spectrograph and was used to detect the spectrally resolved lines. The ICCD detector was operated in the gated mode. The gate delay and width of the ICCD were adjusted so that the spectra, at different time delays after the laser pulse, can be obtained. Data acquisition and analysis were performed with a personal computer.

#191010 - $15.00 USD Received 22 May 2013; revised 6 Jul 2013; accepted 11 Jul 2013; published 22 Jul 2013

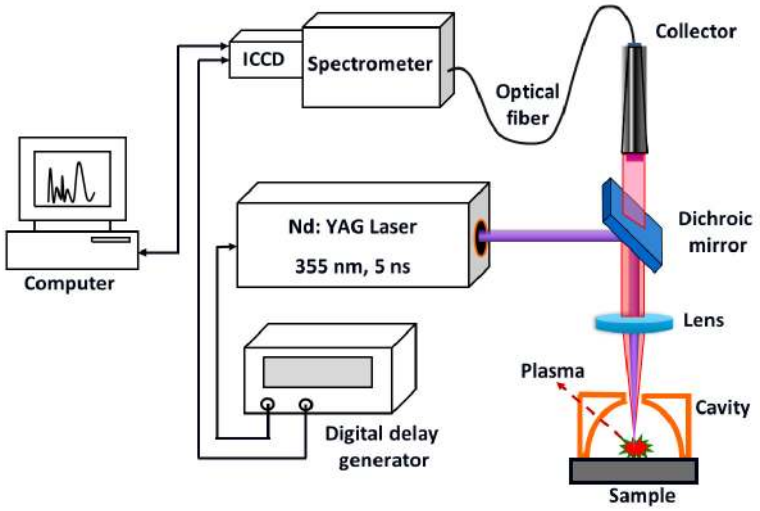

Fig. 1. Schematic diagram of the experimental setup.

Seven steel samples (GSB03-2582-2010, PanGang Group Research Institute Co. Ltd, Sichuan Province, China,) with V, Cr, and Mn concentrations lower than 0.827%, 0.157%, and 2.06%, respectively, as well as matrix element Fe were used in this study. Concentrations of these elements are listed in Table 1 with their standard deviations.

Table 1. Composition of V, Cr, Mn, and Fe elements from the Steel Samples

	Sample No.	No. 1	No. 2	No. 3	No. 4	No. 5	No. 6	No. 7
V	Standard values (%)	0.0090	0.044	0.071	0.158	0.335	0.506	0.821
	Standard deviation (%)	0.0004	0.002	0.002	0.004	0.007	0.004	0.007
Cr	Standard values (%)	0.511	0.080	0.030	0.117	0.171	0.387	0.157
	Standard deviation (%)	0.007	0.003	0.001	0.004	0.004	0.007	0.004
Mn	Standard values (%)	0.072	0.0329	1.22	0.857	0.596	1.46	2.06
	Standard deviation (%)	0.001	0.008	0.01	0.007	0.007	0.02	0.02
Fe	Standard values (%)	96.625	95.115	94.501	94.490	94.286	92.234	90.097
	Standard deviation (%)	0.02	0.02	0.02	0.02	0.02	0.02	0.02

3. Results and discussion

3.1 Time-integrated LIBS of V, Cr, and Mn in the steel samples

First, the time-integrated LIBS spectra of laser-induced V, Cr, and Mn plasmas from the steel samples were measured to demonstrate the intensity enhancement effects of the low concentration elements. As shown in Fig. 2, the emission spectra of V, Cr, and Mn from steel sample No. 7 were obtained in a spectral range of 424–495 nm with (solid curves) and without (short dotted curves) the presence of a hemispherical cavity with a diameter of 5 mm under otherwise the same conditions. The Nd:YAG laser beam was focused to a spot size around 0.42 mm in diameter, with a laser fluence of 42.9 J/cm^2. The gate delay and gate width were 2.5 and 0.5 μs, respectively. The signals were accumulated with consecutive ablations by 20 pulses to reduce the standard deviation. The emission intensities for the Cr (425.43 nm), V (440.85 nm) and Mn (476.64 nm) atomic lines were all obviously enhanced with the presence of the cavity. The transition configurations for the Cr, V and Mn atomic lines are $3d^5(^6S)4s$ - $3d^5(^6S)4p$, $3d^4(^5D)4s$ - $3d^4(^5D)4p$ and $3d^6(^5D)4s$ - $3d^6(^5D)4p$, respectively (where the $3d^5(^6S)4s$, $3d^4(^5D)4s$ and $3d^6(^5D)4s$ are the ground states of the Cr, V and Mn atoms). Transition parameters for the Cr, V, and Mn atomic lines are listed in Table 2.

#191010 - $15.00 USD Received 22 May 2013; revised 6 Jul 2013; accepted 11 Jul 2013; published 22 Jul 2013

Table 2. Transition parameters of the Mn, Cr, and V atomic lines

Element name	Wavelength(nm)	Lower level	Upper level
Mn	476.64	$3d^6(^5D)4s$	$3d^5(^5D)4p$
Cr	425.43	$3d^5(^6S)4s$	$3d^5(^6S)4p$
V	440.85	$3d^4(^5D)4s$	$3d^4(^5D)4p$

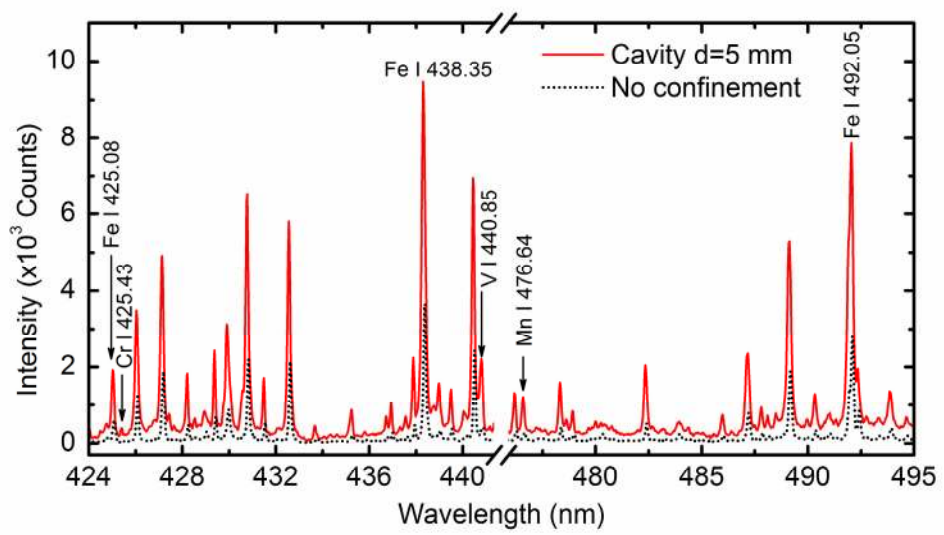

Fig. 2. Time-integrated LIBS spectra of Mn, Cr, and V elements from steel target No. 7 with (solid curve) and without (short dashed curve) the presence of a hemispherical cavity (diameter: 5 mm) at a laser fluence of 42.9 J/cm^2.

3.2 Influence of different cavity diameters

To optimize the cavity dimension in this study, an emission intensity of V I 440.85 nm was obtained from the steel samples, using hemispheric cavities with diameters of 4 (diamond dots and curve), 5 (pentagon dots and curve), 6 (triangle dots and curve), and 7 (circle dots and curve), respectively, as shown in Fig. 3. The ICCD started to acquire spectra from 0.5 μs after the plasma produced, with a gate width of 0.5 μs and a step of 0.5 μs. The intensity of V atomic lines without a cavity (square dots and curve) was also plotted for comparison. Comparing the case with the spatial confinement using the 5 mm hemispheric cavity (pentagon dots and curve) with the case without confinement (square dots and curve), the emission intensity of V I 440.85 nm had no significant difference at a delay time of 1.0 μs. After that, the emission intensity started to increase slowly and then rapidly at delay times from 1.5 to 2.5μs. It decreased quickly after 2.5μs. The strongest enhancement was attained at a delay time of 2.5 μs, reaching an enhancement factor (compared to that without confinement) of about 4.2. Similar results were obtained when adopting cavity diameters of 6 and 7 mm. From a delay time of 3 μs, the emission intensity with the cavity suddenly started to increase linearly, indicating that the reflected shockwave collided with the propagating plasma front at this time. As the cavity size increased, the enhancement effect occurred later and became weaker. The enhancement factors for the cavity sizes of 6 and 7 mm were about 3.1 and 2.87, which were attained at delay times of 4.5 and 5 μs, respectively. It was slightly different for the cavity size of 4 mm. The emission intensity decreased slowly from 0.5 to 1.5 μs, then suddenly started to decrease linearly from 1.5 μs. The cavity was too small, so the reflected shockwave was not able to regularize the plasma due to energy dissipation [28]. The best enhancement was achieved at a delay time of 2.5 μs, reaching an enhancement factor of about 3.9. It can be seen that the cavity with a diameter of 5 mm had the best confinement.

#191010 - $15.00 USD Received 22 May 2013; revised 6 Jul 2013; accepted 11 Jul 2013; published 22 Jul 2013

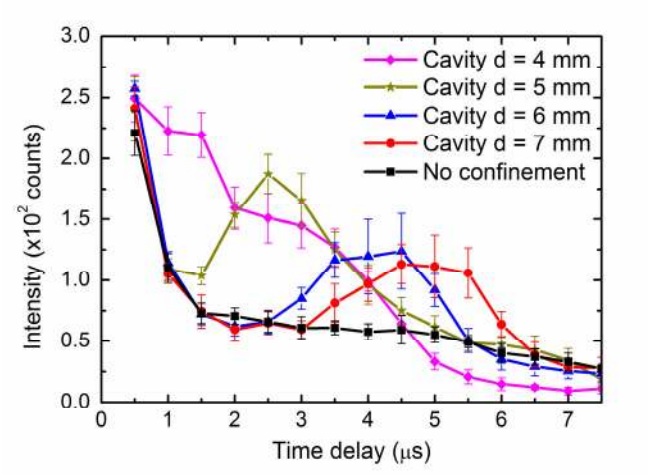

Fig. 3. Emission intensity of V I 440.85 nm with or without confinement by hemispheric cavities of different diameters at a laser fluence of 42.9 J/cm^2.

3.3 The influence of the laser energy

Having selected an appropriate cavity size, the laser fluence was adjusted to further improve the enhancement effects. Figure 4 shows the temporal evolution of the emission intensity from V atomic lines with the presence of the hemispherical cavity under different laser fluences of 37.4, 40.6, 42.9, 44.2, and 46.3 J/cm^2, respectively. The signals were acquired from 0.5 μs after the plasma produced, with a gate width of 0.5 μs and a step of 0.5 μs. As the laser fluence decreased, the time delay for the maximum enhancement appeared at 2, 2.5, 2.5, 2.5, and 3 μs, respectively. A longer delay time for the maximum enhancement was due to the fact that the speed of the shock wave was proportional to the value of the laser fluence [21]. Lower laser fluence produced a slower shock wave which needed longer traveling time to compress the plasma. It can be seen that the best enhancement was obtained at the delay time of 2.5 μs, with a fluence of 42.9 J/cm^2.

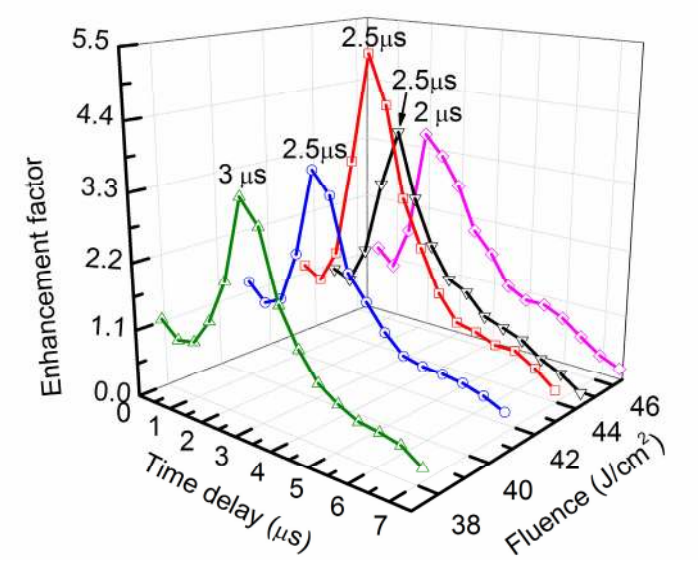

Fig. 4. Emission intensity of the V atomic line (V I with 440.85 nm) as a function of time delay, with the hemispherical cavity (diameter: 5 mm) at laser fluences of 37.4, 40.6, 42.9, 44.2 and 46.3 J/cm^2, respectively.

#191010 - $15.00 USD Received 22 May 2013; revised 6 Jul 2013; accepted 11 Jul 2013; published 22 Jul 2013

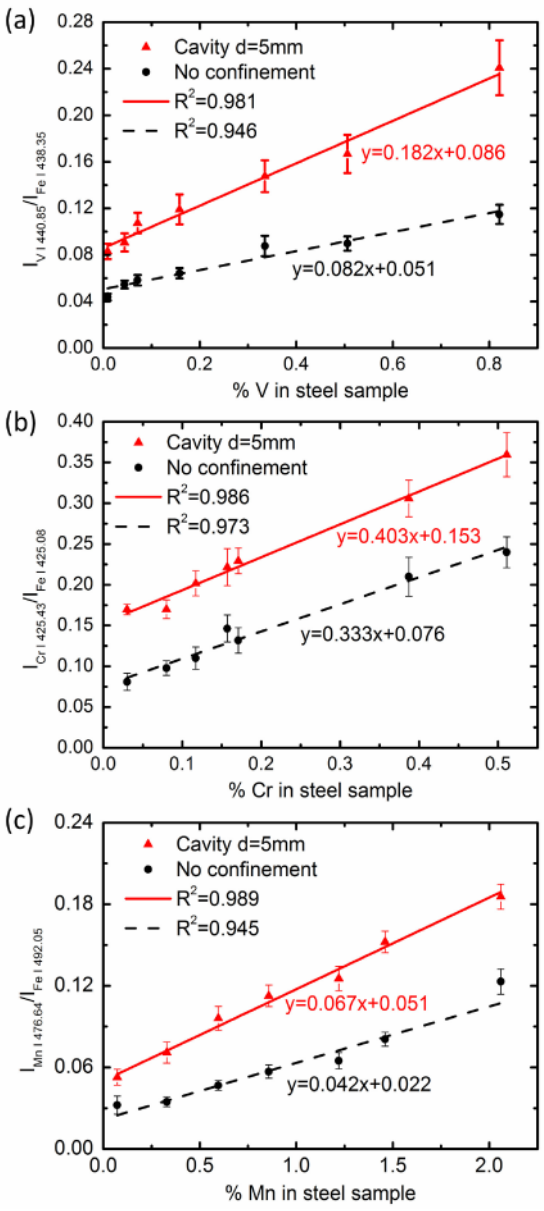

Fig. 5. Calibration curves vs. concentration in steel alloys: (a) V(I) 440.85 nm/Fe(I) 438.35 nm vs. V concentration; (b) Cr(I) 425.43 nm/ Fe(I) 425.08 nm vs. Cr concentration; (c) Mn(I) 476.64 nm/Fe(I) 492.05 nm vs. Mn concentration.

3.4 Calibration curves for V, Cr, and Mn

To avoid a number of experimental parameters that are difficult to measure, the internal standardization method has been used widely in the LIBS, the ratio of the line intensity of a low element to the emission line of the internal standard was measured and plotted as a function of the known concentration ratios in the reference samples. These plots defined the calibration curves that allow quantitative analysis in unknown samples [29]. Based on the results previously described, a combination of 5 mm hemispherical cavity and a laser fluence of 42.9 J/cm^2 have the best confinement effect. The low-concentration elements V, Cr, and

#191010 - $15.00 USD Received 22 May 2013; revised 6 Jul 2013; accepted 11 Jul 2013; published 22 Jul 2013

Mn were chosen to compare their quantitative analyses for cases with and without the 5 mm cavity confinement. Figures 5(a) to 5(c) show the calibration curves for V (0.009–0.821%), Cr (0.03–0.511%), and Mn (0.0329–2.06%). According to the standard concentrations in samples No. 1-7, the relative intensity ratios of line V I 440.85/Fe I 438.35 nm, Cr I 425.43/Fe I 425.08 nm, and Mn I 476.64 nm/Fe I 492.05 nm were plotted as a function of the relative concentration in a linear scale, with (triangle dots and solid curve) and without (circle dots and dashed curve) the cavity, respectively. The emission spectra of the plasma were measured with a delay time of 2.5 μs and a gate width of 0.5 μs. Each point was the average of ten measurements, and each measurement was carried out by accumulating LIBS spectra with 20 laser shots. A calibration curve shows a near straight line, indicating a nearly linear relationship between the emission intensity and the concentration.

From these results, it was calculated that the correlation coefficients of the ratio (R^2) of the V I 440.85/Fe I 438.35 nm with (triangle dots and solid curve) and without (circle dots and dashed curve) the cavity were 0.981 and 0.946, respectively, as shown in Fig. 5(a). The R^2 value of the internal calibration method with V I 440.85/Fe I 438.35 nm was improved by the spatial confinement. Similar results for Cr I 425.43/Fe I 425.08 nm and Mn I 476.64 nm/Fe(I) 492.05 nm without and with cavity were 0.973 and 0.986, 0.945 and 0.989, respectively, were also obtained, as shown in Figs. 5(b) and 5(c).

Therefore, the accuracy of quantitative analysis of low concentration elements, such as V, Cr, and Mn, in steel samples was improved with spatial confinement. In the experiment, a shock wave was produced by the initial explosive pressure along with the plasma generation and spread out as a spherical wave with a high supersonic velocity [30]. When the spherical wave encountered the hemispherical cavity wall, it uniformly reflected and traveled back towards the plasma center. The plasma was compressed and become uniform; therefore, the spectral line intensity was enhanced. As a result, the accuracy of quantitative analysis was improved [27,28].

4. Conclusions

In this work, the accuracy of quantitative analysis was improved by spatial confinement in laser-induced breakdown spectroscopy. The plasma produced by a Nd:YAG laser in air from steel targets was confined by a cavity. A number of elements with low concentrations, such as vanadium (V), chromium (Cr), and manganese (Mn), in the steel samples were investigated. After the optimization of spatial dimension and laser fluence, significant enhancement factors of 4.2, 3.1, and 2.87 in the emission intensity of V, Cr, and Mn lines, respectively, were achieved at a laser fluence of 42.9 J/cm^2 with a hemispherical cavity (diameter: 5 mm). More importantly, the correlation coefficient of the V I 440.85/Fe I 438.35 nm was increased from 0.946 (without the cavity) to 0.981 (with the cavity), and similar results for Cr I 425.43/Fe I 425.08 nm and Mn I 476.64/Fe I 492.05 nm without and with a cavity were 0.973 and 0.986, 0.945 and 0.989, respectively, were also obtained. Therefore, the accuracy of quantitative analysis of low concentration elements such as V, Cr, and Mn in steel samples was improved with spatial confinement. The results of this study provide a new pathway for improving the accuracy of quantitative analysis of LIBS.

Acknowledgment

This research was also financially supported by the National Special Fund for the Development of Major Research Equipment and Instruments (No. 2011YQ160017), and by the National Natural Science Foundation of China (No. 51128501).

#191010 - $15.00 USD Received 22 May 2013; revised 6 Jul 2013; accepted 11 Jul 2013; published 22 Jul 2013